J|A|C|S
COMMUNICATIONS

Published on Web 12/06/2006

Cooperative Jahn-Teller Distortion, Phase Transitions, and Weak Ferromagnetism in the $KCrF_3$ Perovskite

Serena Margadonna* and Georgios Karotsis

School of Chemistry and Centre for Science at Extreme Conditions, University of Edinburgh, Edinburgh EH9 3JJ, U.K.

Received September 26, 2006; E-mail: serena.margadonna@ed.ac.uk

The chemistry of transition-metal oxides has been full of surprises and intriguing structural, electronic, and magnetic phenomena. One of the key ingredients at the origin of these effects is the availability of degenerate electronic orbitals. Whether such orbital degrees-of-freedom actually occur in a material depends on the nature of the atomic ions and the surrounding crystallographic structure. Prominent examples of ions that display active orbital degrees-of-freedom include the Jahn-Teller (JT) Mn^{3+} (d^4) and Cu^{2+} (d^9) ions. For instance, Mn^{3+} is present in many important transition-metal oxides such as $LaMnO_3$, the parent compound of the colossal magnetoresistance manganites. The magnetic behavior of $LaMnO_3$ perovskite is particularly interesting because the cooperative JT distortion (CJTD) is accompanied by A-type antiferromagnetic (AF) spin and C-type orbital (OO) ordering, exemplifying the strong interplay between spin, orbital, and structural ordering phenomena. Similar effects also play a fundamental role in determining the physical properties of non-oxide materials like the pseudocubic perovskite, $KCuF_3$ which behaves as a one-dimensional $S = {}^1/_2$ antiferromagnet.

The ternary fluoride with formula $KCrF_3$ has striking similarities with both $LaMnO_3$ and $KCuF_3$: first, at ambient conditions, it adopts a perovskite-type structure, and second, it incorporates the JT active Cr^{2+} (d^4) ion whose electronic configuration and magnetic response are analogous to those of Mn^{3+} and Cu^{2+}. Very surprisingly, its structural and electronic phase diagrams have not been studied in any detail. Early structural work has reported that $KCrF_3$ adopts a tetragonal structure at room temperature ($a = 4.270$ Å, $c = 4.019$ Å; space group $P4/mmm$),[1] while powder neutron diffraction showed at low temperatures a magnetic transition ($T_N = 40$ K) to an A-type AF structure.[2] Here we report that when we probed the structural and magnetic properties of $KCrF_3$ as a function of temperature ($5 < T < 300$ K), a structurally and magnetically far richer phase diagram than hitherto supposed was revealed. $KCrF_3$ exhibits a series of temperature-induced complex structural and magnetic transitions, and there is strong evidence for the presence of large cooperative JT distortions which are driven by orbital ordering.

The high-resolution synchrotron X-ray powder diffraction profile of $KCrF_3$ at 295 K revealed that its structure was body centered tetragonal ($a = b \approx \sqrt{2}a_p$, $c \approx 2a_p$, where a_p is the lattice constant of the pseudocubic perovskite cell).[3] Analysis with the LeBail pattern decomposition technique resulted in lattice parameters, $a = 6.05230(2)$, $c = 8.02198(4)$ Å, and $a = b > c/\sqrt{2}$ (space group $I4/mcm$). The unit-cell metrics are different from those previously reported but are reminiscent of those in $KCuF_3$.[4] The final Rietveld refinement (Figure 1a) revealed that the CrF_6 octahedra are strongly axially distorted, comprising short Cr−F bonds (2.00549(1) Å) along the c-axis and alternating long (2.294(4) Å) and short (1.986(4) Å) Cr−F bonds in the ab plane (octahedral distortion parameter,[5] $\Delta d = 46.2 \times 10^{-4}$)—this provides compelling evidence for the presence of a CJTD which leads to an antiferrodistortive ordering of the $3d_{3x^2-r^2}$ and $3d_{3y^2-r^2}$ orbitals (OO) in the ab plane.[6] Along the c-axis, the orbital ordering pattern is rotated by 90° in consecutive layers (a-type).

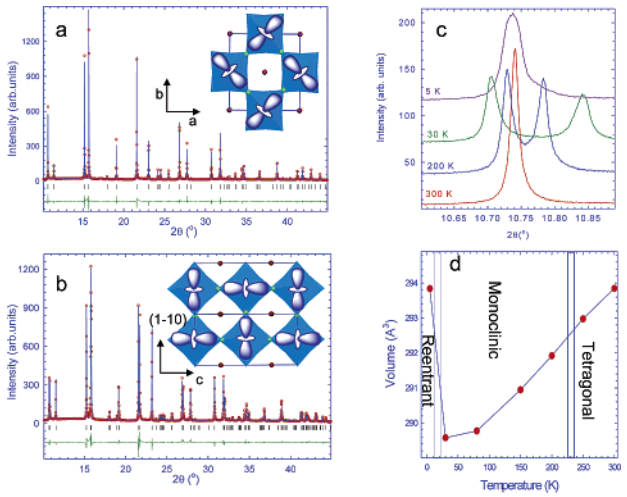

Figure 1. Final observed (○) and calculated (−) synchrotron X-ray diffraction profiles ($\lambda = 0.80160$ Å) for $KCrF_3$ at (a) 295 K ($a = 6.05230(2)$ and $c = 8.02196(3)$ Å, space group $I4/mcm$. Agreement factors of the Rietveld refinement: $R_{wp} = 6.03\%$, $R_{exp} = 4.57\%$) and (b) 150 K ($a = 5.82642(5)$, $b = 5.83517(5)$, and $c = 8.57547(5)$ Å, $\gamma = 93.686(1)°$, space group $I112/m$. Agreement factors of the Rietveld refinement: $R_{wp} = 6.87\%$, $R_{exp} = 5.59\%$). The lower solid lines show the difference profiles and the tick marks show the reflection positions. The insets in panels a and b show the corresponding $3d_{z^2}$ orbital ordering schemes. (c) Selected region of the diffraction profile of $KCrF_3$ showing the temperature evolution of the (110) tetragonal Bragg reflection and its splitting into the monoclinic (002) and (−110) reflections, which eventually merge at low temperature. (d) Temperature evolution of the unit-cell volume as extracted from the Rietveld refinements.

However, on cooling below 250 K, $KCrF_3$ shows a phase transition to a monoclinic structure ($a \approx b < c/\sqrt{2}$) with pronounced CrF_6 octahedral tilting (space group $I112/m$). This is drastically different from the behavior of the $KCuF_3$ analogue whose tetragonal structure is retained down to 4 K[4] and is presumably associated with the reduced tolerance factor of $KCrF_3$ ($\tau = 0.99$). Rietveld refinements show that the alternating long/short (2.296(9)/1.977(8) Å) Cr−F bond ordering and antiferrodistortive $3d_{z^2}$ OO patterns are maintained (Figure 1b), but they now occur in the plane defined by the c-axis and the ⟨1−10⟩ base diagonal and are rotated by 90° in consecutive layers along the ⟨110⟩ direction (Cr−F bond lengths along ⟨110⟩ = 2.01(1) Å). While the ordering motifs are essentially identical to those in the ambient temperature structure, the significant $a^0b^0c^-$ octahedral tilting of 6.9° leads to an increase in the magnitude of the CJTD ($\Delta d = 60.5 \times 10^{-4}$ at 150 K). In addition, a notable feature of the structural model is the presence of two crystallographically independent Cr^{2+} sites with similar coordination environment. Such a situation is very unusual for

10.1021/ja0669272 CCC: $33.50

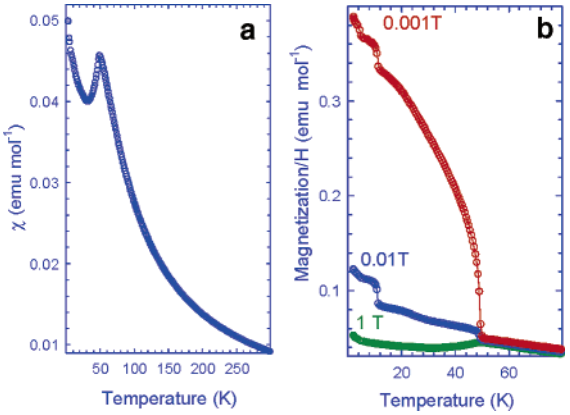

Figure 2. Temperature dependence of (a) the magnetic susceptibility χ (H = 1 T) of $KCrF_3$ (the increase below T_N may arise from paramagnetic impurities) and (b) the (magnetization/field) ratio at selected fields.

simple ABX_3 perovskite-type materials with isovalent B-site cations but is reminiscent of the strongly distorted crystal structure of $NaCuF_3$, in which there are four inequivalent Cu^{2+} sites.[7]

The monoclinic structure remains stable in the temperature range between 200 and 30 K. The *a* and *b* axes decrease gradually on cooling, while the *c*-axis shows a continuous increase (Figure 2S, Supporting Information), reflecting the increase in the degree of octahedral tilting (8.2° at 30 K). However, the lattice response of $KCrF_3$ to further decrease in temperature to 5 K is dramatically different. The diffraction peaks suddenly shift (Figure 1c) implying an abrupt change in the lattice parameters toward values metrically similar to those at 295 K (reentrant-type phase transition) and a sharply reduced monoclinic distortion and octahedral tilting. The diffraction profile at 5 K (Figure 1S) can be indexed with a unit cell: $a = 6.04805(10)$, $b = 6.05376(6)$, and $c = 8.02308(5)$ Å, $\gamma = 89.92(1)°$ (space group $I112/m$, $a \approx b > c/\sqrt{2}$). The alternating long/short Cr−F bond order (2.29(1)/2.00(1) Å) now occurs in the *ab* plane in analogy with the ordering pattern observed at 295 K. In addition, the phase transition to the much less distorted phase is accompanied by an anomalous large volume expansion of ~1.5% (negative thermal expansion), leading to a unit-cell volume at 5 K slightly larger than that at 295 K (Figure 1d).[8] Further cooling below 5 K may induce a complete reentrant phase transition.

$KCrF_3$ was reported to adopt an A-type antiferromagnetic (AF) structure.[2] The molar magnetic susceptibility χ_M measured in an applied field of 1 T clearly shows a well-defined kink on cooling, providing the signature of the onset of long-range AF ordering with a Néel temperature T_N of 46 K (Figure 2a). Above 100 K, the Curie−Weiss law is obeyed with a positive Weiss temperature, $\theta = 2.7(1)$ K implying the existence of ferromagnetic (FM) exchange interactions. The measured $\chi_M T$ at 300 K (2.71 emu K mol^{-1}) gives a value for the effective magnetic moment, $\mu_{eff} = 4.7\ \mu_B$ which is consistent with that for a high-spin Cr^{2+} ion. We also measured the field dependence of the field-cooled magnetization (FCM) in the temperature range between 80 and 2 K (Figure 2b). In a small applied field of 1 mT, the magnetization shows a sharp increase exactly at the same temperature at which the cusp in the susceptibility occurs. The spontaneous magnetization continues to increase on cooling but two further discontinuities in the FCM are evident at 11 and 4 K. The spontaneous magnetic moment approaches a value of 4 emu Oe mol^{-1} at 2 K. The signature of the transitions at lower temperatures disappears upon increasing the value of the applied field. These observations point toward a description of the low-temperature magnetic behavior of $KCrF_3$ as that of a weak ferromagnet.

The magnetic properties of $KCrF_3$ can be rationalized if we consider the nature of the exchange interactions within and between the CJTD/OO planes for both tetragonal and monoclinic structures. In analogy with the weak FM $LaMnO_3$ ($\mu_s = 0.18\ \mu_B/Mn^{3+}$ ion),[9] the superexchange interactions within the OO planes give rise to FM exchange between neighboring Cr^{2+} spins, accounting for the observed positive Weiss temperature. We note that there is no evidence of the tetragonal-to-monoclinic structural transition in the temperature dependence of the susceptibility. Moreover, AF coupling between the OO FM planes can account for the long-range AF order observed below 46 K. The origin of the accompanying weak FM is presumably associated with the presence of small-spin canting, arising by either single-ion anisotropy effects and/or the Dzyaloshinsky−Moriya interaction and related to the small out-of-plane inclination of the $3d_{z^2}$ orbitals along the ⟨110⟩ stacking direction of the monoclinic phase. The additional features in the magnetization at 11 and 4 K could be intrinsic in nature as they occur in the same temperature range as the re-entrant structural transition and could reflect small changes in the spin-canting angle.

In conclusion, we have found that the perovskite-type fluoride $KCrF_3$ shows a strong interplay of lattice, orbital, and spin degrees-of-freedom, which give rise to a complex temperature-dependent structural and magnetic response. In $KCrF_3$, the CJTD are accompanied by orbital ordering and weak ferromagnetism, which is reminiscent of what is observed in $LaMnO_3$. It will be intriguing to explore within this family of fluorides the synthesis of $Cr^{2+/3+}$ structural and electronic analogues of the CMR $Mn^{3+/4+}$ oxides, especially as the monoclinic structure of $KCrF_3$ can support metal (charge) ordering.

Acknowledgment. S.M. thanks J. P. Attfield for discussions, the Royal Society for a Dorothy Hodgkin Research Fellowship, and the ESRF for provision of beamtime.

Supporting Information Available: Tables of extracted structural parameters from the Rietveld refinements at 295, 150, and 5 K; plots of the Rietveld refinement at 5 K, the temperature dependence of the lattice constants, and magnetic hysteresis M vs H at 2 K. This material is available free of charge via the Internet at http://pubs.acs.org.

References

(1) Edwards, A. J.; Peacock, R. D.; *J. Chem. Soc.* **1959**, 4126.
(2) Scatturin, V.; Corliss, L.; Elliott, N.; Hastings, J. *Acta Crystallogr.* **1961**, *14*, 19. Yoneyama, S.; Hirakawa, K. *J. Phys. Soc. Jpn.* **1966**, *21*, 183.
(3) $KCrF_3$ samples were prepared by the reaction of stoichiometric quantities of KF and CrF_2 pressed into pellets and contained in sealed Mo cells inside evacuated quartz tubes at 550 °C for 2 days with one intermediate grinding. For the X-ray diffraction measurements, the sample was sealed in a thin-wall capillary, 0.5 mm in diameter. Data ($\lambda = 0.80160$ Å, $2\theta = 5-50°$, $\Delta(2\theta) = 0.001°$) were collected at various temperatures with the high-resolution powder diffractometer on beamline ID31 at the ESRF, Grenoble, France. Data analysis was performed with the GSAS suite of Rietveld programs. Field-dependent magnetization measurements were performed between 2 and 300 K with a Quantum Design SQUID magnetometer.
(4) Hutchings, M. T.; Samuelsen, E. J.; Shirane, G.; Hirakawa, K. *Phys. Rev.* **1969**, *188*, 919. Buttner, R. H.; Maslen, E. N.; Spadaccini, N. *Acta Crystallogr., Sect. B: Struct. Sci.* **1990**, *46*, 131.
(5) Lufaso, M. W.; Woodward, P. M. *Acta Crystallogr., Sect. B: Struct. Sci.* **2004**, *60*, 10.
(6) High-resolution synchrotron X-ray powder diffraction is an indirect probe of the nature of orbital ordering, and techniques such as resonant X-ray scattering and X-ray linear dichroism are needed to give direct information about orbital occupancy.
(7) Kaiser, V.; Otto, M.; Binder, F.; Babel, D. *Z. Anorg. Allg. Chem.* **1990**, *585*, 93.
(8) The low-temperature reentrant phase transition appears to be sensitive to the cooling protocols employed in the course of the diffraction experiments.
(9) Skumryev, V.; Ott, F.; Coey, J. M. D.; Anane, A.; Renard, J.-P.; Pinsard-Gaudart, L.; Revcolevschi, A. *Eur. Phys. J. B* **1999**, *11*, 401.

JA0669272